Real-time, subsecond, multicomponent breath analysis by Optical Parametric Oscillator based Off-Axis Integrated Cavity Output Spectroscopy

Denis D. Arslanov,* Koen Swinkels, Simona M. Cristescu, and Frans J. M. Harren

Life Science Trace Gas Research Group, Molecular and Laser Physics, Institute for Molecules and Materials, Radboud University, P.O. Box 9010, NL-6500 GL Nijmegen, the Netherlands

*D.Arslanov@science.ru.nl

Abstract: Breath analysis is an attractive field of research, due to its high potential for non-invasive medical diagnostics. Among others, laser-based absorption spectroscopy is an excellent method for the detection of gases in exhaled breath, because it can combine a high sensitivity with a good selectivity, and a high temporal resolution. Here, we use a fast-scanning continuous wave, singly-resonant Optical Parametric Oscillator (wavelength range between 3 and 4 μm, linewidth 40 MHz, output power > 1 W, scanning speed 100 THz/s) with Off-Axis Integrated Cavity Output Spectroscopy for rapid and sensitive trace gas detection. Real-time, low-ppbv detection of ethane is demonstrated in exhaled human breath during free exhalations. Also, simultaneous, real-time multi-component gas detection of ethane, methane and water was performed in exhaled breath using a wide spectral coverage over 17 cm^{-1} in 1 second. Furthermore, real-time detection of acetone, a molecule with a wide absorption spectrum, was shown in exhaled breath, with a sub-second time resolution (0.4 s).

OCIS codes: (140.0140) Lasers and laser optics; (190.4410) Nonlinear optics, parametric processes; (190.4970) Parametric oscillators and amplifiers; (190.4975) Parametric processes; (280.1415) Biological sensing and sensors.

References and links

1. T. H. Risby and F. K. Tittel, "Current status of midinfrared quantum and interband cascade lasers for clinical breath analysis," Opt. Eng. **49**(11), 111123 (2010).
2. W. Miekisch, J. K. Schubert, and G. F. E. Noeldge-Schomburg, "Diagnostic potential of breath analysis--focus on volatile organic compounds," Clin. Chim. Acta **347**(1-2), 25–39 (2004).
3. T. H. Risby, "Volatile organic compounds as markers in normal and diseased states," in *NATO ASI Series, Disease markers in exhaled breath: basic mechanisms and clinical applications*, N. Marczin and M. H. Yacoub, eds. (IOS, 2002), pp.113–122.
4. T. H. Risby and S. F. Solga, "Current status of clinical breath analysis," Appl. Phys. B **85**(2-3), 421–426 (2006).
5. C. Wang and P. Sahay, "Breath Analysis Using Laser Spectroscopic Techniques Breath Biomarkers, Spectral Fingerprints, and Detection Limits," Sensors (Basel Switzerland) **9**(10), 8230–8262 (2009).
6. B. Buszewski, M. Kesy, T. Ligor, and A. Amann, "Human exhaled air analytics: biomarkers of diseases," Biomed. Chromatogr. **21**(6), 553–566 (2007).
7. A. Artlich, B. Jónsson, M. Bhiladvala, P. A. Lönnqvist, and L. E. Gustafsson, "Single breath analysis of endogenous nitric oxide in the newborn," Biol. Neonate **79**(1), 21–26 (2001).
8. V. H. Tran, P. C. Hiang, M. Thurston, P. Jackson, C. Lewis, D. Yates, G. Bell, and P. S. Thomas, "Breath analysis of lung cancer patients using an electronic nose detection system," IEEE Sens. J. **10**(9), 1514–1518 (2010).
9. G. Berden and R. Engeln, *Cavity Ring-Down Spectroscopy: Techniques and Applications* (Wiley, 2009).
10. S. M. Cristescu, S. T. Persijn, S. te Lintel Hekkert, and F. J. M. Harren, "Laser-based systems for trace gas detection in life sciences," Appl. Phys. B **92**(3), 343–349 (2008).
11. R. Lewicki, J. H. Doty 3rd, R. F. Curl, F. K. Tittel, and G. Wysocki, "Ultrasensitive detection of nitric oxide at 5.33 μm by using external cavity quantum cascade laser-based Faraday rotation spectroscopy," Proc. Natl. Acad. Sci. U.S.A. **106**(31), 12587–12592 (2009).
12. V. Spagnolo, A. A. Kosterev, L. Dong, R. Lewicki, and F. K. Tittel, "NO trace gas sensor based on quartz-enhanced photoacoustic spectroscopy and external cavity quantum cascade laser," Appl. Phys. B **100**(1), 125–130 (2010).

#154407 - $15.00 USD Received 8 Sep 2011; revised 15 Oct 2011; accepted 30 Oct 2011; published 11 Nov 2011

13. D. D. Arslanov, S. M. Cristescu, and F. J. M. Harren, "Optical parametric oscillator based off-axis integrated cavity output spectroscopy for rapid chemical sensing," Opt. Lett. **35**(19), 3300–3302 (2010).
14. B. J. Orr and Y. He, "Rapidly swept continuous-wave cavity-ringdown spectroscopy," Chem. Phys. Lett. **512**(1-3), 1–20 (2011).
15. E. R. Crosson, K. N. Ricci, B. A. Richman, F. C. Chilese, T. G. Owano, R. A. Provencal, M. W. Todd, J. Glasser, A. A. Kachanov, B. A. Paldus, T. G. Spence, and R. N. Zare, "Stable isotope ratios using cavity ring-down spectroscopy: determination of $^{13}C/^{12}C$ for carbon dioxide in human breath," Anal. Chem. **74**(9), 2003–2007 (2002).
16. M. L. Silva, D. M. Sonnenfroh, D. I. Rosen, M. G. Allen, and A. O'Keefe, "Integrated cavity output spectroscopy measurements of NO levels in breath with a pulsed room-temperature QCL," Appl. Phys. B **81**(5), 705–710 (2005).
17. J. Manne, O. Sukhorukov, W. Jäger, and J. Tulip, "Pulsed quantum cascade laser-based cavity ring-down spectroscopy for ammonia detection in breath," Appl. Opt. **45**(36), 9230–9237 (2006).
18. I. Ventrillard-Courtillot, T. Gonthiez, C. Clerici, and D. Romanini, "Multispecies breath analysis faster than a single respiratory cycle by optical-feedback cavity-enhanced absorption spectroscopy," J. Biomed. Opt. **14**(6), 064026 (2009).
19. H. Dahnke, D. Kleine, P. Hering, and M. Murtz, "Real-time monitoring of ethane in human breath using mid-infrared cavity leak-out spectroscopy," Appl. Phys. B **72**, 971–975 (2001).
20. D. Halmer, S. Thelen, P. Hering, and M. Mürtz, "Online monitoring of ethane traces in exhaled breath with a difference frequency generation spectrometer," Appl. Phys. B **85**(2-3), 437–443 (2006).
21. M. J. Thorpe, D. Balslev-Clausen, M. S. Kirchner, and J. Ye, "Cavity-enhanced optical frequency comb spectroscopy: application to human breath analysis," Opt. Express **16**(4), 2387–2397 (2008).
22. J. H. Shorter, D. D. Nelson, J. B. McManus, M. S. Zahniser, S. R. Sama, and D. K. Milton, "Clinical study of multiple breath biomarkers of asthma and COPD (NO, CO_2, CO and N_2O) by infrared laser spectroscopy," J. Breath Res. **5**(3), 037108 (2011).
23. G. N. Rao and A. Karpf, "External cavity tunable quantum cascade lasers and their applications to trace gas monitoring," Appl. Opt. **50**(4), A100–A115 (2011).
24. K. R. Parameswaran, D. I. Rosen, M. G. Allen, A. M. Ganz, and T. H. Risby, "Off-axis integrated cavity output spectroscopy with a mid-infrared interband cascade laser for real-time breath ethane measurements," Appl. Opt. **48**(4), B73–B79 (2009).
25. S. Persijn, F. Harren, and A. van der Veen, "Quantitative gas measurements using a versatile OPO-based cavity ringdown spectrometer and the comparison with spectroscopic databases," Appl. Phys. B **100**(2), 383–390 (2010).
26. A. K. Y. Ngai, S. T. Persijn, G. von Basum, and F. J. M. Harren, "Automatically tunable continuous-wave optical parametric oscillator for high-resolution spectroscopy and sensitive trace-gas detection," Appl. Phys. B **85**(2-3), 173–180 (2006).
27. J. B. Paul, L. Lapson, and J. G. Anderson, "Ultrasensitive absorption spectroscopy with a high-finesse optical cavity and off-axis alignment," Appl. Opt. **40**(27), 4904–4910 (2001).
28. G. S. Engel, W. S. Drisdell, F. N. Keutsch, E. J. Moyer, and J. G. Anderson, "Ultrasensitive near-infrared integrated cavity output spectroscopy technique for detection of CO at 1.57 μm: new sensitivity limits for absorption measurements in passive optical cavities," Appl. Opt. **45**(36), 9221–9229 (2006).
29. L. S. Rothman, I. E. Gordon, A. Barbe, D. Chris Benner, P. F. Bernath, M. Birk, V. Boudon, L. R. Brown, A. Campargue, J.-P. Champion, K. Chance, L. H. Coudert, V. Dana, V. M. Devi, S. Fally, J.-M. Flaud, R. R. Gamache, A. Goldman, D. Jacquemart, I. Kleiner, N. Lacome, W. J. Lafferty, J.-Y. Mandin, S. T. Massie, S. N. Mikhailenko, C. E. Miller, N. Moazzen-Ahmadi, O. V. Naumenko, A. V. Nikitin, J. Orphal, V. I. Perevalov, A. Perrin, A. Predoi-Cross, C. P. Rinsland, M. Rotger, M. Šimečková, M. A. H. Smith, K. Sung, S. A. Tashkun, J. Tennyson, R. A. Toth, A. C. Vandaele, and J. Vander Auwera, "The HITRAN 2008 molecular spectroscopic database," J. Quant. Spectrosc. Radiat. Transf. **110**(9-10), 533–572 (2009).
30. T. T. Groot, P. M. van Bodegom, F. J. M. Harren, and H. A. J. Meijer, "Quantification of methane oxidation in the rice rhizosphere ^{13}C-labelled methane," Biogeochemistry **64**(3), 355–372 (2003).
31. D. D. Arslanov, M. Spunei, A. K. Y. Ngai, S. M. Cristescu, I. D. Lindsay, S. T. Persijn, K. J. Boller, and F. J. M. Harren, "Rapid and sensitive trace gas detection with continuous wave optical parametric oscillator-based wavelength modulation spectroscopy," Appl. Phys. B **103**(1), 223–228 (2011).
32. A. K. Y. Ngai, S. T. Persijn, I. D. Lindsay, A. A. Kosterev, P. Groß, C. J. Lee, S. M. Cristescu, F. K. Tittel, K.-J. Boller, and F. J. M. Harren, "Continuous wave optical parametric oscillator for quartz-enhanced photoacoustic trace gas sensing," Appl. Phys. B **89**(1), 123–128 (2007).
33. S. W. Sharpe, T. J. Johnson, R. L. Sams, P. M. Chu, G. C. Rhoderick, and P. A. Johnson, "Gas-phase databases for quantitative infrared spectroscopy," Appl. Spectrosc. **58**(12), 1452–1461 (2004).
34. J. King, A. Kupferthaler, K. Unterkofler, H. Koc, S. Teschl, G. Teschl, W. Miekisch, J. Schubert, H. Hinterhuber, and A. Amann, "Isoprene and acetone concentration profiles during exercise on an ergometer," J. Breath Res. **3**(2), 027006 (2009).

1. Introduction

Breathing is an important process that provides our body with oxygen but also removes carbon dioxide from the body. It is a complex process of gas exchange in the alveoli by diffusion of gasses over the lung capillaries. Our exhaled breath consist of 15-18% O_2, 4-6%

#154407 - $15.00 USD Received 8 Sep 2011; revised 15 Oct 2011; accepted 30 Oct 2011; published 11 Nov 2011

CO_2, 5% H_2O, ppmv-levels of H_2 and CO, around 0.5-1 ppmv (parts-per-million by volume, 1×10^{-6}) NH_3, several hundreds of ppbv (parts-per-billion by volume, 1×10^{-9}) of acetone, methanol, ethanol, and many other volatile organic compounds (VOCs) at ppbv and pptv level (parts-per-trillion by volume, 1×10^{-12}) level [1]. The source of exhaled gases can be of exogenous origin via inspiration air or the skin, via ingested foods or beverages; it can be produced in the mouth, nose, sinuses and airways, or can come from the blood via the alveolar-capillary junction in the lungs [1]. In general, the amount and composition of exhaled VOCs vary per subject and within a subject over time. Especially, diseases or metabolic disorders will change the production of VOCs. Produced locally, they are spread over the entire body and reach the lungs via the blood circulation. Hence, breath analysis is an attractive and promising field for diagnostics and monitoring in medicine. It is non-invasive and safe, and allows easy sample collection, even from very sick, old people or neonates. It provides physicians and patients with real-time results, which is important for early disease diagnostics.

The last decade, a large amount of clinical and scientific studies are performed using breath analysis. Nowadays, a number of fundamental problems still needs attention in breath analysis; in particular with regard to preparation and storage of breath samples, proper real-time breath monitoring, and correlating disease with the exhaled VOCs [2–4]. There are more than thousand different gases found in exhaled breath [5], but only detectors for O_2, CO_2, CO, H_2, methane (CH_4) and nitric oxide (NO) are widely used in commercial devices. Yet, there are other known indicators that relate to a certain diseases or disorders. For example, acetone (C_3H_6O) is related to diabetes, dietary fat losses, congestive heart failure, brain seizure and lung cancer; ethane (C_2H_6) is related to lipid peroxidation and oxidative stress; methane is associated with intestinal problems and colonic fermentation [5,6]. However, the detailed formation mechanism for some of these indicators is not well understood. Hence, it is important to quantify amount and timing of gaseous indicators in relation to a disease, detecting their sensitivity at trace gas concentration level.

In the past, several detection methods were used for trace gas measurements in biomedical applications, ranging from mass spectrometry [6], gas chromatography [6], chemiluminescence [7], electronic nose [8], to different laser-based spectroscopic methods [5,9–14]. As many molecular gases have strong absorption in the mid-IR wavelength region, it is advantageous to use laser absorption spectroscopy; it is an excellent method for highly sensitive and selective detection of VOCs. While a gas cell is filled with a sample gas, the wavelength of the laser is tuned over an absorption line of the gas under investigation. According to Lambert-Beer's law, the transmitted laser intensity, detected on a photodetector, depends on the absorption strength of the gas at that wavelength, the gas concentration and the path length within the sampling cell. As each molecule has its own specific absorption spectrum in the mid-IR wavelength region, it is possible to determine gas concentration and to distinguish selectively molecules in a complex gas mixture.

A disadvantage of the breath analysis is that the gas composition of exhaled breath varies within one exhalation. The actual exhaled breath consist of contributions from different parts of the respiratory system: nose, mouth, upper/lower trachea, or the alveolar-capillary junction; hence, the gas concentration in exhaled breath varies over time. High finesse optical cavity methods are often used for breath studies. However, they are not always fulfilling real-time analysis criterion [15–17], have a narrow wavelength tuning range [18], do not have a continuous coverage of the wavelength tuning range [19], or use a low power laser source [20]. In addition there is a spectroscopic problem, larger VOCs have many more ro-vibational transitions than simpler molecules such as CH_4. Their rotational lines are not resolved; therefore, the spectrum is broad and structureless. Thus, a tunable laser system over a wide wavelength range is needed to properly detect such VOCs.

Usually, laser spectroscopy deals with the detection of one molecule as function of time. Although, there are systems which allow measuring several gases simultaneously, they are often complex, expensive [21], and contain several laser sources [22], or have a relatively slow wavelength tuning scheme [23]. Here we aim to overcome these issues and built, based

#154407 - $15.00 USD Received 8 Sep 2011; revised 15 Oct 2011; accepted 30 Oct 2011; published 11 Nov 2011

on Optical Parametric Oscillator spectroscopy, a sensitive and selective trace gas detector with a sub-second time resolution, and tunable over a wide wavelength range for simultaneous multicomponent detection.

In our recent work [13] we have shown that fast scanning continuous wave Singly-Resonant Optical Parametric Oscillator (SRO) incorporated with Off-Axis Integrated Cavity Output Spectroscopy (OA-ICOS) is a powerful tool for rapid and sensitive trace gas detection. A detection of 50 pptv of ethane (C_2H_6) measured in 0.25 s. was determined [13]. The noise-equivalent detection limit of 25 pptv/$Hz^{1/2}$ is found to be almost in 20 times better than the one determined in [24] of 0.48 ppbv/$Hz^{1/2}$ for ethane when using OA-ICOS with an interband cascade laser. This definitely proves the suitability of our setup to perform human exhaled breath ethane measurements. The sensitivity of OA-ICOS is comparable to other spectroscopic techniques such as Cavity Ring Down Spectroscopy (CRDS) and Photoacoustic (PA) spectroscopy, known for their high-quality detection limits [5,25,26]. The advantage of Integrated Cavity Output Spectroscopy (ICOS) is that the recording time can be much shorter than for CRDS or PA, because it is not a resonant technique and there are no slow response elements (such as microphones). Here, the developed setup gives us the opportunity to evolve a real-time breath analysis system, measuring ethane during free exhalation; perform real-time multicomponent detection of water, ethane and methane with a time resolution of 0.1 s; and detect acetone with a time resolution of 0.4 s in exhaled human breath taking advantage of the fast, wide spectral coverage (17 cm^{-1} recorded in 1 s) of the OPO.

2. Experimental setup

2.1 Optical parametric oscillator Integrated Cavity Output Spectroscopy (ICOS)

The experimental setup of the SRO pumped by a fiber-amplified diode laser based ICOS is shown in Fig. 1 and was described earlier in detail [13]. Here only a short description is given. An 80 mW multisection Distributed Bragg Reflector (DBR) diode laser (Eagleyard Photonics) with an output wavelength of 1082 nm seeds a 30 m long double-clad Yb-doped fiber (F), which is pumped by a 25 W fiber-coupled 976 nm cw diode-laser bar (FP). Two isolators (not shown) are used to prevent feedback, while a quarter-wave plate and half-wave plates (not shown) are used for polarization control and for gauging of a total output power of up to 7.5 W. The gain section within the DBR laser is used to generate the output wavelength, while the phase and Bragg sections are used to tune the output wavelength by applying the currents through the resistors attached to these sections. By synchronized tuning of the phase and the Bragg section of the DBR laser, 3 cm^{-1} wide mode-hop-free tuning ranges can be achieved at scanning rates of 1 kHz. Slower scanning rates will cover a wider wavelength range (e.g. 5 cm^{-1} at 100 Hz). The effective output linewidth of the DBR laser is 40 MHz. The cw SRO cavity consists of a four-mirror bow-tie ring design. The pump beam is focused in a quasi-phase matched 5% MgO-doped periodically poled lithium niobate crystal (PP-MgO-LN) with seven poling periods ranging from 28.5 to 31.5 μm. The crystal was placed in an oven capable of maintaining temperatures from 20 °C to 200 °C with a stability of 0.02 °C. A 400 μm thick YAG intracavity etalon (E) was inserted into the SRO cavity for the frequency stabilization. For course wavelength generation, the appropriate crystal poling period and temperature are chosen, after that DBR laser tuning was used for the fast mode-hop-free tuning of the output wavelength of the OPO. The wavelength was monitored with a wavelength meter (WA-1000, Burleigh; not shown), whereas during experiments Fabry-Perot etalon fringe pattern was used to measure the accurate relative wavelength. Up to 1.2 W of idler output was produced, at a pump power of 7.5 W.

For OA-ICOS, the high-finesse optical cavity (calculated finesse value F = 15700) consists of a pair of highly reflective, 2 inch diameter, concave mirrors (R=99.98% at 3.3μm, ROC = 1 m, Nova-Wave Technology) mounted on a 60 cm long stainless steel tube (inner diameter 40 mm) with two inlets/outlets for gas exchange. The transmitted laser intensity was focused via a lens on the fast thermoelectrically cooled photodetector (PD) with a time response of 20 ns (HgCdZnTe, VIGO Systems PDI-2TE-4). ICOS is more robust technique

#154407 - $15.00 USD Received 8 Sep 2011; revised 15 Oct 2011; accepted 30 Oct 2011; published 11 Nov 2011

than the CRDS and less technically demanding. Similar to CRDS, the laser light is used to excite high finesse cavity modes, but the technique can be used without limitations concerning ring-down time or mode matching between the laser frequency and the free spectral range (FSR) of the cavity. In contrast to cw CRDS, the laser light is not locked on each cavity mode but swept over the gas absorption line. Off-axis injection of the laser beam into the ICOS cell increases effectively the cavity length; hence, the FSR of the cavity collapses and laser light can be coupled into the cell at many cavity modes, simultaneously. In a successful off-axis alignment many cavity modes exist under every molecular transition line, which decreases the mode noise [9,27,28].

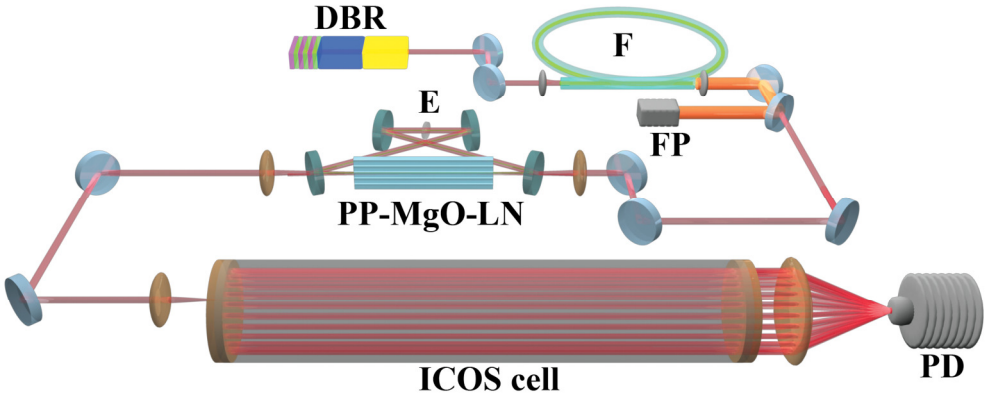

Fig. 1. Experimental setup of the Optical Parametric Oscillator pumped by a fiber amplified DBR laser incorporated with ICOS setup. *DBR*- Distributed Bragg Reflector diode laser, *F*- double clad Yb-doped fiber, *FP*- fiber pump diode laser bar, *PP-MgO-LN*- MgO-doped periodically poled lithium niobate crystal, *E*- intra-cavity etalon, *ICOS cell*- integrated cavity output spectroscopy cell, *PD*- photodetector.

2.2 On-line breath measurements

Figure 2 shows the scheme of the experimental setup for real-time breath analysis. The ICOS cell was pumped by a vacuum pump with a capacity of up to 230 ml/s (Edwards, model ESDP 30). This pump speed was chosen for a sub-second refreshing time of the cell, taking into account the flow rate (exhaled breath, 14 l/min) and the cell volume (1 l, effective volume 200 ml at 200 mbar pressure. Using smaller cell volumes or lower pressures will result in lower pump speeds, but can also lead to reduced sensitivities.

Lab air was supplied as a background gas in the experiments in cases where high water, methane etc. concentrations did not influence the results. However, for precise measurements pure nitrogen gas was used. To deliver a gas sample into the cell a mouthpiece connected to a two-way non-rebreathing valve in T-shape configuration (Hans Rudolph inc.) was used. A small portion of the sample went to the conventional capnograph (Capnomac Ultima, Datex Ohmeda), which provided real-time carbon dioxide concentrations in exhaled breath.

#154407 - $15.00 USD Received 8 Sep 2011; revised 15 Oct 2011; accepted 30 Oct 2011; published 11 Nov 2011

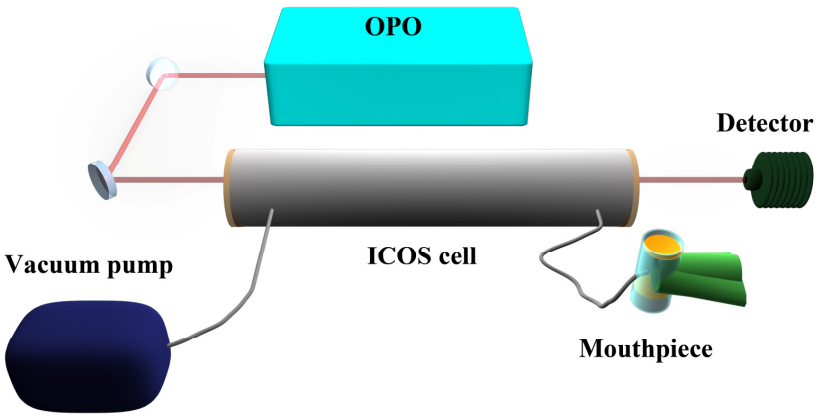

Fig. 2. Experimental setup for the real-time breath sampling. *OPO*- Optical Parametric Oscillator pumped by a fiber amplified diode laser, *Vacuum pump*- capacity 230 ml/s (Edwards, model ESDP 30), *ICOS cell*- Integrated Cavity Output Spectroscopy cell, *Mouthpiece*- mouthpiece with a two-way non-rebreathing valve in T-shape configuration (Hans Rudolph inc.), *Detector*- HgCdZnTe photodetector (VIGO Systems PDI-2TE-4).

3. Results and discussion

3.1 Real-time detection of ethane in exhaled breath

Rapid and sensitive trace gas detection was performed by measuring ethane in exhaled human breath. Figure 3(a) shows the 200 mbar broadened spectra for 1 ppbv ethane and 2% water using HITRAN 2008 database [29] in the wavelength range between 2970 cm^{-1} and 3005 cm^{-1}; the wavelength region around 2997 cm^{-1} was used for C_2H_6 detection, because it is free of H_2O interference. Figure 3(b) represents the same data in the range of 2996.4 cm^{-1} to 2997.6 cm^{-1} adding 5% carbon dioxide and 1.7 ppmv methane. The figure shows that ethane is spectroscopically well separated from the other gases, which are present at high concentrations in exhaled breath.

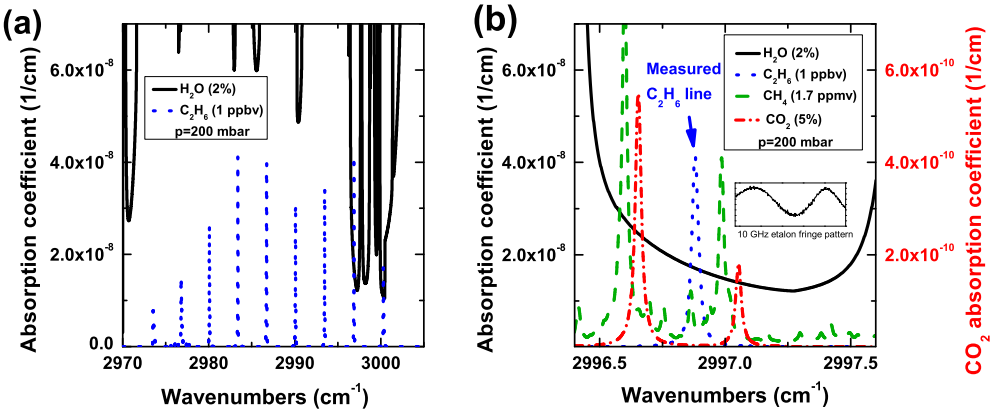

Fig. 3. Simulated spectra at a pressure of 200 mbar based on HITRAN 2008 database [17] for: (Panel a) 2% water (black solid line) and 1 ppbv ethane (blue dotted line) in the wavelength range 2970-3005 cm^{-1}; (Panel b) 2% water (black solid line, left vertical scale), 1 ppbv ethane (blue dotted line, left vertical scale), 1.7 ppmv methane (green dashed line, left vertical scale) and 5% carbon dioxide (red dot-dashed line, right vertical scale) in the wavelength range 2996.4-2997.6 cm^{-1}. Figure insertion shows etalon fringe pattern with free spectral range of 10 GHz for the fine wavelength tracking during long-term measurements.

#154407 - $15.00 USD Received 8 Sep 2011; revised 15 Oct 2011; accepted 30 Oct 2011; published 11 Nov 2011

Although the absorption cross section of ethane is much higher than that of methane at 2996.9 cm^{-1}, methane is present in the atmosphere at a relatively high concentration of 1.7 ppmv [30]; Fig. 3(b) indicates that absorption coefficients of 1 ppbv ethane and 1.7 ppmv methane are nearly equal at this wavelength. This shows that for precise measurements during long-term experiments the wavelength has to be controlled. However, the wavemeter (Wavemeter WA-1000 has a speed of 1 Hz) cannot follow the high scanning speeds, up to 100 THz/s, of the OPO [31]. Therefore, we measured the relative wavelength by tracking an etalon fringe pattern (see insertion in Fig. 3(b)); a 1.5 cm long, air-spaced etalon with a free spectral range of 10 GHz was used for this.

Real-time breath sampling of ethane was performed over the ethane absorption line at 2996.9 cm^{-1} (Fig. 3(b)) during free exhalation in multiple breaths. It is known that air contains ethane at a concentration level typically of between 1 and 10 ppbv [24]. Our lab air, which was used as background gas, contained ethane concentrations around 6 ppbv at the time of the measurements. Ethane data were taken at a laser scanning rate of 1 kHz over the absorption line and averaged over 256 scans. This resulted in a sampling time of 0.25 seconds. Figure 4(a) represents the dynamics of ethane (black solid line, left vertical scale) and carbon dioxide (red dotted line, right vertical scale) concentrations for a non-smoking subject. No difference was found in the ethane concentration between air and exhaled breath. Figure 4(b) shows similar measurements for a person half an hour after he smoked a cigarette. Here, the exhaled breath contained ethane at a concentration level of 11 ppbv, 5 ppbv higher than the background ethane concentration. That higher concentrations can be found is breath is seen in Fig. 5, the exhaled breath of a smoker is showed over a period of 35 minutes, directly after smoking a sigarette; even after 40 minutes an elevated level of ethane is present in exhaled breath.

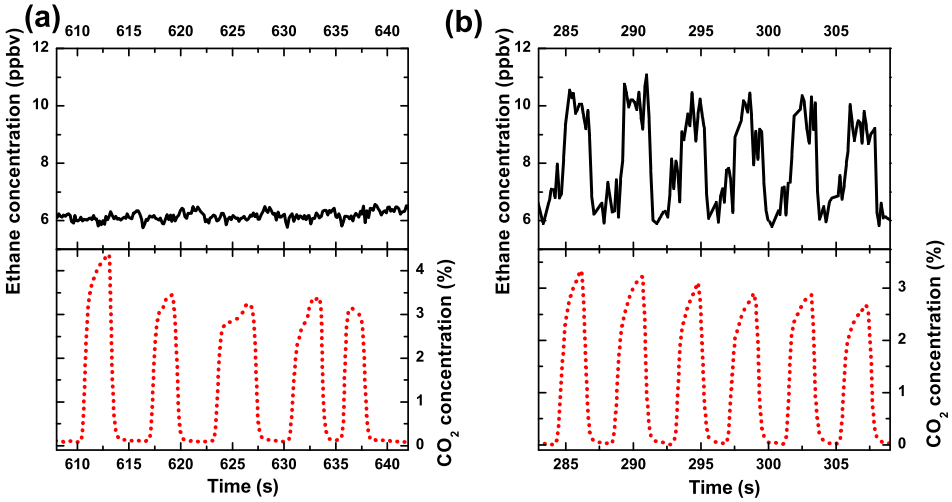

Fig. 4. Concentration dynamics of ethane during free exhalation in multiple breaths (black solid line, left vertical scale, measured with OPO based OA-ICOS) and carbon dioxide (red dotted line, right vertical scale, measured with capnograph (Capnomac Ultima, Datex Ohmeda): (Panel 4a) non-smoking subject, (Panel 4b) smoking subject half an hour after a cigarette was smoked.

#154407 - $15.00 USD Received 8 Sep 2011; revised 15 Oct 2011; accepted 30 Oct 2011; published 11 Nov 2011

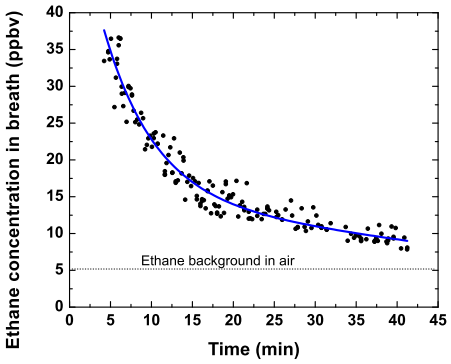

Fig. 5. Long-term measurements of ethane, exhaled by a smoking subject. Every dot corresponds to a concentration in a single, free exhalation. The blue solid line is an exponential fit of the experimental data. Dashed line at the bottom of the figure shows the level of ethane in air during measurements. Zero time corresponds to the moment when the last cigarette was smoked.

3.2 Real-time multi-component gas detection in exhaled breath

Using a spectral region within one mode-hop-free tuning range of the laser, containing absorption spectra of several gases, allows detection of multiple gases at high temporal resolution. Here, the spectroscopic range around 2997 cm^{-1} was used for simultaneous detection of ethane, methane and water in exhaled breath. Figure 6 represents the calculated spectra of these gases at this wavelength region. Experimentally, ethane (blue dotted line) was measured at the top of the 2996.9 cm^{-1} line, methane (green dashed line) at the top of the 2997 cm^{-1} and water (black solid line) at the top of the 2997.5 cm^{-1} line. Figure 7 shows the real-time measurements of concentration of C_2H_6 (blue dotted line), CH_4 (green dashed line), H_2O (black solid line) and CO_2 (red dash-dotted line) during free exhalation of three different subjects (panel a, b and c) at a time resolution of 0.13 s (256 scan averages at a 2 kHz repetition rate). Figure 7(a) shows the elevated level of ethane and methane in exhaled breath of the first subject, while Fig. 7(b) shows only the high level of methane for the second subject, and Fig. 7(c)- neither methane, nor ethane in exhaled breath of the third subject.

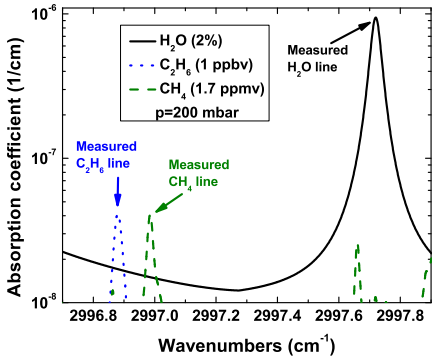

Fig. 6. Calculated spectra for water 2% (black solid line), ethane 1 ppbv (blue dotted line) and methane 1.7 ppmv (green dashed line) in the wavelength range between 2996.7 and 2997.9 cm^{-1} at a pressure of 200 mbar.

#154407 - $15.00 USD Received 8 Sep 2011; revised 15 Oct 2011; accepted 30 Oct 2011; published 11 Nov 2011

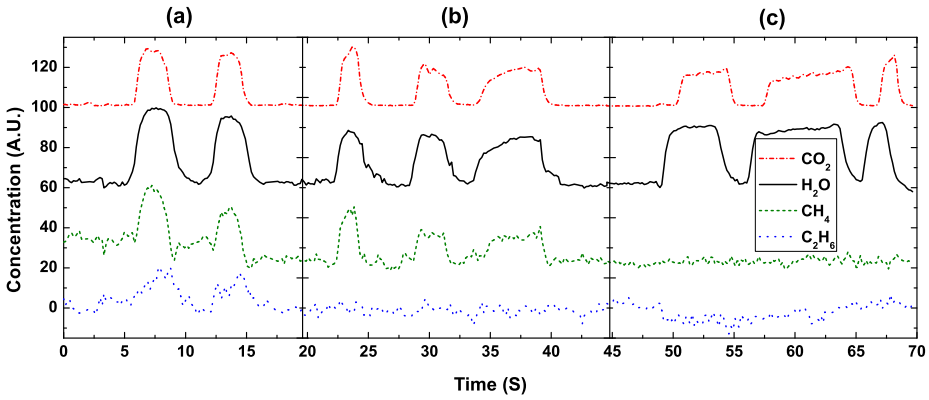

Fig. 7. Real-time multicomponent detection of water (black solid line), methane (green dashed line), carbon dioxide (red dash-dotted line) and ethane (blue dotted line) during free exhalation for three different persons: The first person (Panel 7a) shows elevated levels for both methane and ethane, while the second person (Panel 7b) shows only elevated level of methane, and person three (Panel 7c) shows neither elevated levels for methane nor ethane.

3.3 Combining fast detection with a wide spectral coverage

Often, interesting absorption lines of different gases are found to be spectroscopically far from each other. Since the typical tuning range of narrowband laser sources is limited, a multi-component gas measurement is either not possible, or requires additional time to change the wavelength (e.g. by temperature), in order to detect another gas compound. In our setup, apart from a (maximum) 5 cm^{-1} mode-hop-free tuning range of the multi-section DBR laser, an overall 16.5 cm^{-1} tuning range, including mode hops, can be achieved [32]. By varying the current offsets of Bragg and phase section in the pump DBR diode laser mode hops in the pump laser can be avoided up to a tuning range of 5 cm^{-1}, a pump mode hop will induce a mode hop in the signal frequency and thus in the idler frequency. By scanning the pump laser at higher frequencies the total tuning range is considerably reduced to 2 cm^{-1}, the thermal expansion and thermal capacity in the phase and Bragg section is limiting this.

In contrast to the wide tuning range, with mode hops, shown earlier [32], in which a scan of 16.5 cm^{-1} was recorded in 2 min, we demonstrate here a quasi-mode-hope-free tuning over 17 cm^{-1} (2947-2964 cm^{-1}) in just 1 s (Fig. 8). The recorded spectrum consists of eight mode-hop-free regions of about 2 cm^{-1} width, which were merged together creating wide spectral coverage. Each of eight segments in Fig. 8(b) represents the result of a 128 averages recorded at a 1-kHz scanning rate of the laser each with a recording time of 0.13 s, and with a total recording time of 1 s for the complete 17 cm^{-1} wide spectrum. This spectrum (Fig. 8(b)) is found to be in good agreement with the simulated spectrum using the HITRAN 2008 database [29], for a mixture of 1% water and 2 ppmv methane (Fig. 8(a)).

#154407 - $15.00 USD Received 8 Sep 2011; revised 15 Oct 2011; accepted 30 Oct 2011; published 11 Nov 2011

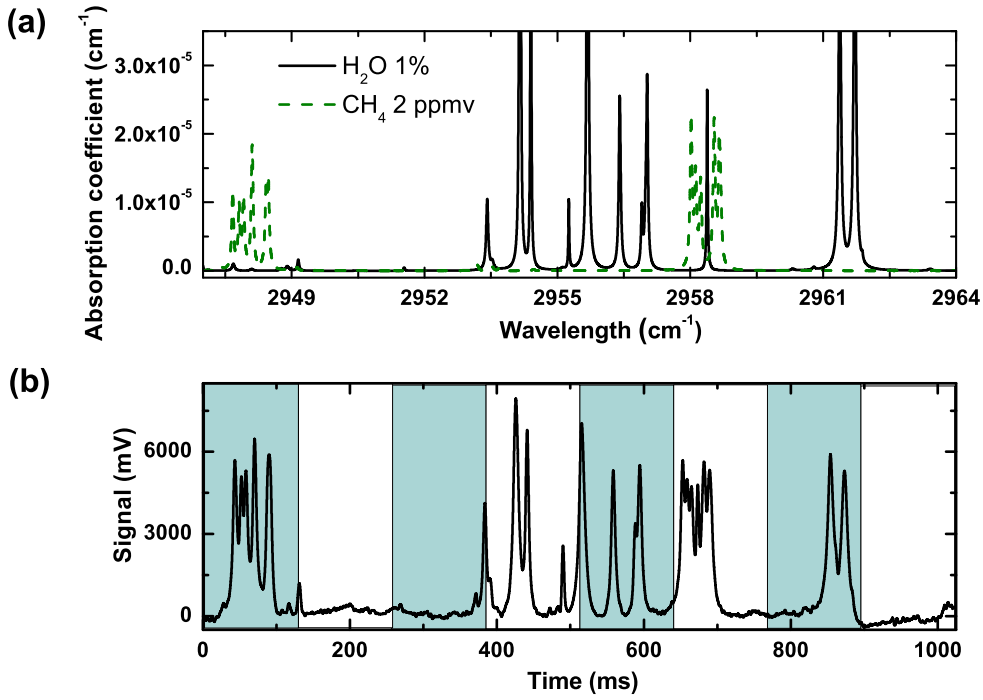

Fig. 8. (Panel a) Simulated spectra for 1% water (black solid line) and 2 ppmv methane (green dashed line) in the wavelength range between 2947 and 2964 cm^{-1}. (Panel b) A 17 cm^{-1} long recorded spectrum of air in 1 s. The spectrum consists of eight mode-hop-free regions of about 2 cm^{-1} width. Each of eight mode-hop-free regions represents the result of 128 averages at a 1-kHz scanning rate and corresponds to certain current offsets for the Bragg and phase sections of the DBR laser. The recorded spectrum is found to be also in good agreement with the simulated spectrum shown on Fig. 8(a).

3.4 Detection of acetone

It is generally known that larger molecules have broad absorption features, due to large amount of vibrational transitions and closely spaced rotational lines. It is, therefore, a challenge to measure larger VOCs with narrowband laser absorption spectroscopy. On the other hand, broadband laser spectroscopy does not yield a high sensitivity and high spectral resolution and can, therefore, hardly applied for breath analysis. Here, we demonstrated that a wide spectrum can be recorded in 1 s time scale. This opens the possibility to detect larger molecules such as acetone with a high spectral and time resolution. Figure 9 shows the simulated spectra for water, methane and acetone in the 2969-2972 cm^{-1} wavelength region at 50 and 500 mbar, using the HITRAN 2008 [29] and PNNL [33] databases. Applying lower pressures in the detection cell will reduce the spectral interference of acetone with water, but consequently it reduces also the detection limit, because the absorption depends proportionally on the amount of acetone molecules present (i.e. pressure).

#154407 - $15.00 USD Received 8 Sep 2011; revised 15 Oct 2011; accepted 30 Oct 2011; published 11 Nov 2011

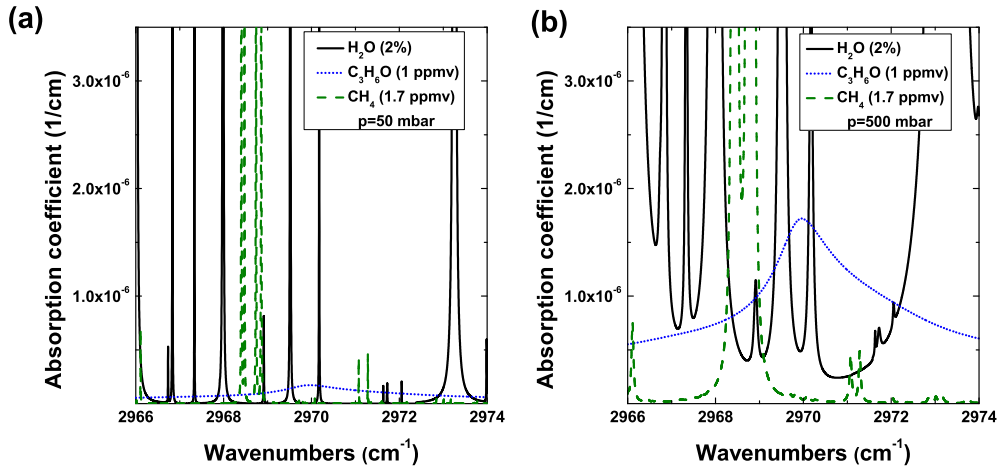

Fig. 9. Simulated spectra for 2% water (black solid line), 1 ppmv acetone (blue dotted line) and 1.7 ppmv methane (green dashed line) in the 2966-2974 cm^{-1} wavelength range for 50 mbar pressure (Panel a) and 500 mbar pressure (Panel b).

Figure 10 shows a real-time scan detecting acetone in exhaled breath in the wavelength range between 2967 cm^{-1} and 2973 cm^{-1}. Figure 10(a) represents spectra of lab air (upper blue line) and exhaled air (bottom red line). The result of subtraction of the exhaled breath spectrum from lab air is shown in Fig. 10(b), as the red line shows the fit with a Voigt profile. The wide absorption feature in the figure belongs to acetone, while other thinner lines are mostly water and methane lines. A scanning rate of the OPO of 1 kHz was used for these measurements. The total scan consists of three mode-hop-free regions. The data shown are the result of 128 scan averages for each of three mode-hop-free regions with a total recording time of 0.4 s.

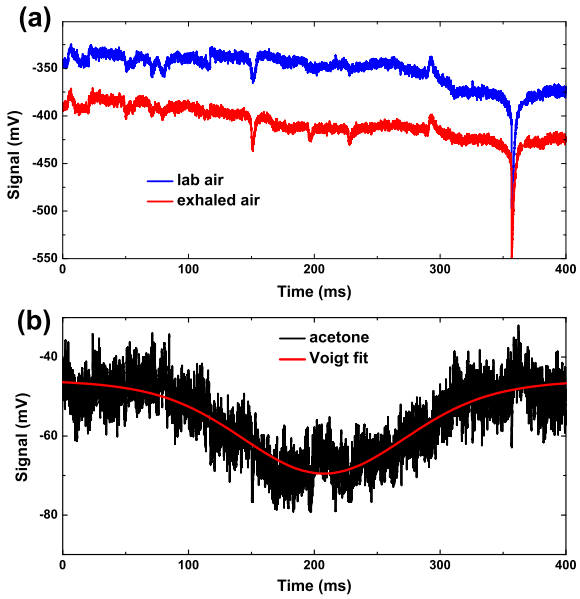

Fig. 10. Real-time measurements of acetone in exhaled human breath. Panel a: Upper blue line indicates a spectrum of lab air, the lower, red line shows exhaled human breath. Panel b: Black line represents the result of subtraction of both lines from panel a. The red curve is the fit with a Voigt profile of the spectrum.

#154407 - $15.00 USD Received 8 Sep 2011; revised 15 Oct 2011; accepted 30 Oct 2011; published 11 Nov 2011

The acetone concentration in the exhaled breath was measured to be 1 ppmv, based on performed calibration measurements (not shown), which leads to a detection limit of acetone of 100 ppbv. This detection limit can be improved by using a detector with better signal to noise ratio than the one we used during our experiments (HgCdZnTe, VIGO Systems PDI-2TE-4). Since typical adult exhaled breath concentrations are around 600 ppb [34], the equipment can be used for the real-time measurements of acetone in exhaled breath.

4. Conclusions

The cw OPO offers high power (>1 W), narrow linewidth and wide wavelength coverage in the wavelength range between 3 and 4 μm, where many molecules have strong absorption lines. Compared with other sources of coherent radiation in the mid-IR, such as quantum cascade lasers and difference frequency generation (low output power of mW or even μW range), it is able to perform an excellent sensitivity for these gasses. This makes the OPO an attractive source for the laser-based absorption spectroscopy. In addition, OA-ICOS is a robust technique, insensitive for temperature fluctuations and mechanical vibrations and provides a sensitivity comparable to other techniques such as CRDS and PA. Furthermore, one of its biggest advantages is that the recording time depends only on the laser scanning speed, which can be as fast as 1 ms or less, for a single scan over a few cm^{-1}. Here, we have demonstrated that the combination of OPO and OA-ICOS is powerful for rapid and sensitive trace gas detection. It allowed real-time detection of ethane in exhaled human breath at low-pppbv level. Simultaneous multi-component gas detection of ethane, methane and water was performed in exhaled breath in real time at a time resolution of 0.1 s. Wide spectral coverage was recorded over 17 cm^{-1} in 1 second, which resulted in the detection of acetone in exhaled breath at sub-second time resolution (0.4 s). A noteworthy feature is the ability to perform real-time multicomponent trace gas detection in exhaled human breath even for larger VOCs, which is an important step forward in breath analysis.

Acknowledgments

This research was financially supported by the IOP Photonic Devices PD 55 “On-chip integrated NH3 human gas sensor” project. The authors would like to thank Cor Sikkens and Peter Claus (Radboud University Nijmegen, the Netherlands) for the technical help to complete the experiments.

#154407 - $15.00 USD Received 8 Sep 2011; revised 15 Oct 2011; accepted 30 Oct 2011; published 11 Nov 2011